Zhong, G., and Peng, X., 2021, Transport and accumulation of plastic litter in submarine canyons—The role of gravity flows: Geology, v. 49, https://doi.org/10.1130/G48536.1

Transport and accumulation of plastic litter in submarine canyons – the role of gravity flows

Guangfa Zhong[1] and Xiaotong Peng[2]

[1]State Key Laboratory of Marine Geology, Tongji University, Shanghai 200092, China

[2]Institute of Deep Sea Science and Engineering, Chinese Academy of Sciences, Hainan 572000, China

This file includes:

Supplementary Background and Methods

Supplementary Figure DR1

Supplementary Table DR1

SUPPLEMENTARY BACKGROUND AND METHODS

Geological background

The northwestern continental margin of the South China Sea (SCS) between Hainan and the Xisha Islands (Fig. 1A) is ENE-orientated, and consists of a flat and wide continental shelf and a relatively steep and rugged continental slope from northwest to southeast. The Xisha Trough, a 430-km-long, roughly E-W-extending submarine canyon system, obliquely cuts across the continental slope. Numerous submarine canyons, named collectively "Xishabei Canyons" (GMGS, 2015), are developed in the relatively steep (3-15°) upper continental slope to the north and as the tributaries of the Xisha Trough (Fig. 1A).

The studied submarine canyon is located between longitudes of 111.86° and 112.10° and latitudes of 18.10° and 18.64° in the east of the Xishabei Canyons (Fig. 1A-B). The roughly N-S extending canyon is approximately 60 km long, 2.2-8.3 km wide and 50-880 m

deep. It commences at 350 m water depth in the outer shelf that is approximately 150 km away from the nearest coast, and extends southward to 2350 m deep in the continental slope, where it merges with the Xisha Trough (Fig. 1A). The shelf-indented and headless submarine canyon consists, from north to south, of a 20-km-long, wide and gently-sloping (average slope = 2°) upper reach, an 8-km-long, narrow, steep (average slope = 6°) and rugged middle reach, and a 32-km-long, wide and flat (average slope = 0.8°) lower reach (Figs. 1B, DR1).

Oceanographical background

It is generally suggested that the SCS contains three-layers of western boundary currents (WBC), which are the upper layer, the intermediate, and the deep WBCs, respectively (Su, 2004; Wang et al., 2011; Tian and Qu, 2012; Zhou et al., 2017; Wang et al., 2019; Zhu et al., 2019). On the northern SCS margin, the upper layer and deep WBCs are cyclonic and flow southwestward, while the intermediate WBC is anticyclonic and flows northeastward (Fig. 1A). The depth of the interface between the upper layer and intermediate WBCs is approximately 500-1000 m, and the depth of the interface between the intermediate and deep WBCs is about 2000 m (Qu et al. 2006; Lan et al., 2013; Zhao et al., 2014; Zhou et al., 2017). On the northern shelf of the SCS, there are year-round currents, including the seasonally reversed Guangdong Coastal Current (GCC, southwestward in winter and northeastward in summer) in the near-shore area and the northeastward SCS Warm Current mainly straddling between 200-400 m isobaths in the outer shelf to shelf-break region (Fig. 1A; Guan, 1978; Guan and Fang, 2006). In addition, the northern SCS margin is frequently attacked by typhoons (storms) and develops world-known strong internal waves, which facilitate cross-shelf transport and diapyncal mixing, respectively (Tian et al., 2009; Alford et al., 2015; Zhou et al., 2017; Xie et al., 2018).

Data and methods

Manned submersible dive observations and footage data, dive based bathymetric profiles, multibeam bathymetric data, and a piston core were available.

Seven dives—one on May 23, 2018 (Dive 78), three on July 5, 18, and 19, 2019 (Dives159 and 172-173), and the remaining three on March 11-13, 2020 (Dives 227-229)—were conducted during three cruises using the manned submersible SHENHAIYONGSHI with R/V TANSUOYIHAO affiliated to the Institute of Deep-Sea Science and Engineering, Chinese Academy of Sciences (Figs. 1B, 2A-B). The 2018 dive covered a 7.8-km-long distance roughly along the canyon thalweg between 1896 m water depth on the downstream end of Scour 2 and 1435 m water depth in the upper reach of the long stepped chute (Figs. 1B and DR1). This dive provided general information on the geomorphology and litter distribution in the stepped chute and the end scours. In this dive, we unexpectedly encountered some litter piles in the scours (Fig. 1B, Peng et al. 2019). Thereafter, the 2019 and 2020 dives were successively made to specifically investigate the distribution of litter accumulations in the scours (Figs. 2-3).

Four sets of video footage were collected in each dive using high quality camera systems mounted respectively at the front, port, starboard, and bottom of the submersible. The data were used to investigate the occurrence of benthic litter, locate the litter piles and measure their sizes.

We used the video footage along selected longitudinal and transverse dive transects (Figs. 3, DR1) to count the number of scattered litter items (not including those in the litter piles) on each snapshot. The areas commonly covered by two consecutive snapshots were marked to avoid counting the litter items inside the common area twice. The counting results were expressed in terms of the number of litter items per snapshot (nlps, one snapshot convers around 10 m×7m area) disregarding particle size. In this counting exercise, litter

items larger than 10 cm were able to be identified in the footage, which represents the cutoff value for the size of the recognizable litter items. Areas of high litter density ($\geqslant$ 4 nlps) were further delineated (Figs. 2A-B, 3).

The ranges of individual litter piles were determined by recording the locations of the submersible in crossing. Orientations of the litter piles were determined by their alignments relative to the tracks of the submersible. The apparent lengths and widths of the litter piles were measured by the amount of crossing displacement of the submersible. Laser marker points and specific litter items with known size were used as references to estimate the heights of the litter piles. All known litter piles were estimated for their length, average width, average height, and volume (Table DR1). These estimates have an error up to 20-30% as evaluated by repeat observations of certain litter piles. In addition, the time-lapse dive observations provide us a unique opportunity to investigate the temporal-spatial variations of the litter accumulations.

One 27-cm-long piston core was collected from Scour 1 in Dive 228, and was sampled at 1 cm interval for grain size analysis using a laser particle-size analyzer to understand the nature of bottom sediment (Fig. 4).

Multibeam bathymetric data covering the submarine canyon investigated were collected in the 2018 dive expedition using the EM122 multibeam acquisition system mounted on the R/V TANSUOYIHAO. The data were used for guiding the dives in the submarine canyon, and revealing the geomorphologic details of the canyon in a precision up to 6-12 m for the target range of 1000-2000 m water depth.

SUPPLEMENTAL REFERENCES

Alford, M.H., Peacock, T., MacKinnon, J.A., Nash, J.D., Buijsman, M.C., Centuroni, L.R., et al., 2015, The formation and fate of internal waves in the South China Sea: Nature, v. 521, p. 65-69.

GMGS (Guangzhou Marine Geological Survey), 2015, Atlas of geology and geophysics of the South China Sea: Beijing, China Navigation Publications Press, 116 p.

Guan, B., 1978, The warm current in the South China Sea — A current flowing against the wind in winter in the open sea off Guangdong Province: Oceanologia et Limnologia Sinica, v. 9, p. 117–127 (in Chinese with English abstract).

Guan, B., and Fang, G., 2006, Winter counter-wind currents off the southeastern China coast: A review: Journal of Oceanography, v. 62, p. 1-24.

Lan, J., Zhang, N., and Wang, Y., 2013, On the dynamics of the South China Sea deep circulation: Journal of Geophysical Research: Oceans, v. 118, p. 1206-1210.

Peng, X., Dasgupta, S., Zhong, G., Du, M., Xu, H., Chen, M., Chen, S., Ta, K., and Li, J., 2019, Large debris dumps in the northern South China Sea: Marine Pollution Bulletin, v. 142, p. 164-168.

Qu, T, Girton, J. B., and Whitehead, J. A., 2006, Deepwater overflow through Luzon Strait: Journal of Geophysical Research, v. 111, C01002.

Su, J., 2004, Overview of the South China Sea circulation and its influence on the coastal physical oceanography outside the Pearl River Estuary: Continental Shelf Research, v. 24, p. 1745-1760.

Tian, J., and Qu, T., 2012, Advances in research on the deep South China Sea circulation: Chinese Science Bulletin, v. 57, p. 1827-1832.

Tian, J., Yang, Q., and Zhao, W., 2009, Enhanced diapycnal mixing in the South China Sea: Journal of Physical Oceanography, v.39, p. 3191-3203.

Wang, D., Wang, Q., Cai, S., Shang, X., Peng, S., Shu, Y., Xiao, J., Xie, X., Zhang, Z., Liu, Z., Lan, J., Chen, D., Xue, H., Wang, G., Gan, J., Xie, X., Zhang, R., Chen, H., and Yang, Q., 2019, Advances in research of the mid-deep South China Sea circulation: Science China Earth Sciences, v. 62, p. 1992-2004.

Wang, G., Xie, S.-P., Qu, T., and Huang, R. X., 2011, Deep South China Sea circulation: Geophysical Research Letter, v. 38, L05601.

Xie, X., Liu, Q., Zhao, Z., Shang, X., Cai, S., Wang, D., and Chen, D., 2018, Deep sea currents driven by breaking internal tides on the continental slope: Geophysical Research Letters, v. 45, p. 6160-6166.

Zhao, W., Zhou, C., Tian, J., Yang, Q., Wang, B., Xie, L., and Qu, T., 2014, Deep water circulation in the Luzon Strait: Journal of Geophysical Research: Oceans, v.119, 790-804.

Zhou, C., Zhao, W., Tian, J., Yang, Q., and Qu, T., 2014, Variability of the Deep-Water Overflow in the Luzon Strait: Journal of Physical Oceanography, v. 44, p. 2972-2986.

Zhou, C., Zhao, W., Tian, J., Zhao, X., Zhu, Y., Yang, Q., and Qu, T., 2017, Deep Western Boundary Current in the South China Sea: Scientific Reports, v. 7, 9303.

Zhu, Y., Sun, J., Wang, Y., Li, S., Xu, T., Wei, Z., and Qu, T., 2019, Overview of the multi-layer circulation in the South China Sea: Progress in Oceanography, v. 175, p. 171-182.

Supplementary Figure DR1: Dive-based bathymetric and corresponding litter density profiles along the 2018 dive track. nlps, number of the scattered litter items per snapshot. See Fig. 2B for profile location.

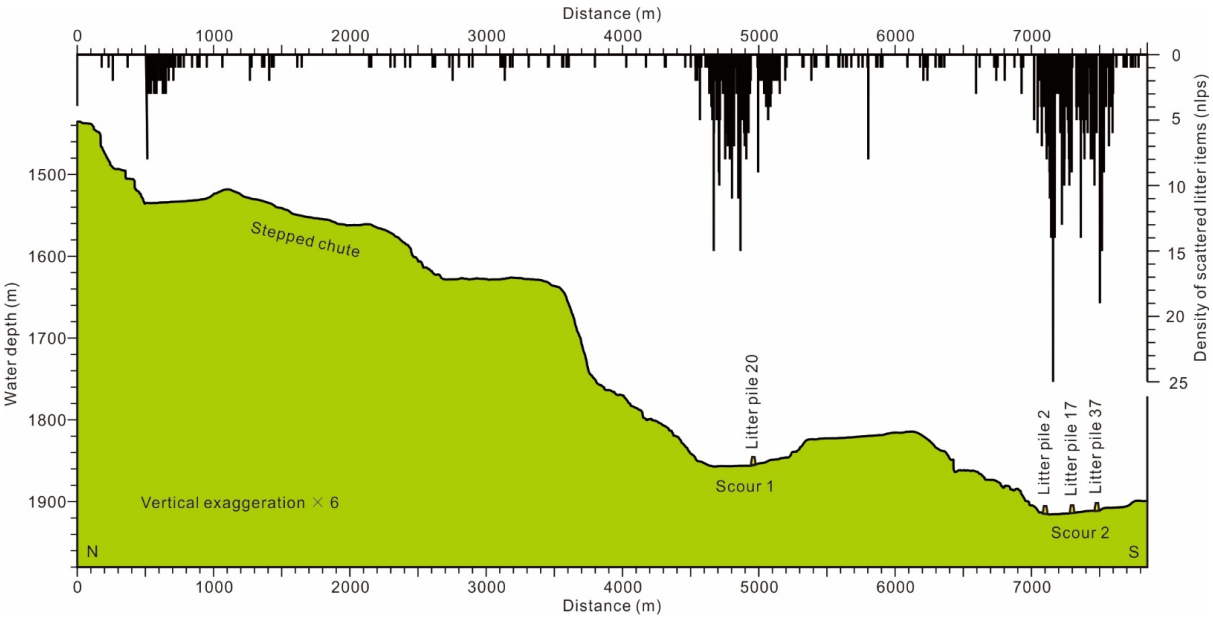

Supplementary Table DR1: Summary of the locations, dimensions and orientations of the litter piles delineated.

Litter pile No.	Longitude (ºE)	Latitude (ºN)	Orientation	Length (m)	Avg. width (m)	Avg. height (m)	Volume (m^3)	Dives
Small scour in the step chute								
1	111.90555	18.44897	N56E	6	2.5	0.3	4.5	159
2	111.90555	18.44881	N38W	8	3.5	0.5	14	159
3	111.90560	18.44869	N60E	5	2	0.3	3	159
Scour 1								
1	111.90758	18.42253	N13E	20	2	0.2	8	228
2	111.90768	18.42229	N8E	5	0.5	0.1	0.3	228
3	111.90774	18.42218	N6E	18	4	0.4	28.8	228
4	111.90791	18.42209	N48W	9	6	0.8	43.2	228
5	111.90800	18.42200	N58W	5	2	0.2	2	228
6	111.90870	18.42199	N86W	2	1	0.1	0.2	179
7	111.90916	18.42192	N-S	12	1	0.1	1.2	228
8	111.90804	18.42183	N54W	4	1.5	0.2	1.2	228
9	111.90796	18.42181	N3E	7	1.5	0.3	3.2	228
10	111.90766	18.42177	N8E	10	2	0.1	2	228
11	111.90921	18.42176	N26W	15	2	0.2	6	228
12	111.90904	18.42172	N35E	12	2	0.2	4.8	78
13	111.90817	18.42166	N79W	8	2.5	0.3	6	228
14	111.90890	18.42163	N63E	5	1	0.2	1	179
15	111.90894	18.42160	N66E	4.5	3	0.2	2.7	179
16	111.90820	18.42159	N83E	12	3	0.2	7.2	228
17	111.90909	18.42146	N40W	8	2	0.2	3.2	179
18	111.90962	18.42136	N26W	6	1.2	0.3	2.2	179
19	111.90920	18.42134	N22W	5	1	0.2	1	179
20-S1*	111.90896	18.42148	N56E	22	3	0.5	33	179
20-S2	111.90907	18.42139	N28E	6	3.5	0.4	8.4	179
20-S3	111.90907	18.42133	N12W	14	1.5	0.2	4.2	179
20-S4	111.90914	18.42128	N32W	7	3	0.5	10.5	179
21-S1	111.90897	18.42156	N18W	29	2	0.2	11.6	179
21-S2	111.90891	18.42131	N7E	18	2	0.3	10.8	179
22	111.90883	18.42125	N24E	15	2.5	0.3	11.3	179
23	111.91052	18.42094	N30W	10	3	0.5	15	228

24	111.90948	18.42079	N28E	3	0.8	0.2	0.5	78
25	111.90930	18.42049	N62E	4	1.5	0.2	1.2	228
26	111.91027	18.41961	N65W	10	3.5	1	35	173
Scour 2								
1	111.91468	18.40932	NS	6	2	0.2	2.4	227
2	111.91337	18.40906	N47W	9	2.5	0.4	9	78
3	111.91340	18.40879	N72W	9	2	0.2	3.6	173
4	111.91340	18.40832	N54W	6	1.2	0.2	1.4	173
5	111.91340	18.40823	N56W	8	2.5	0.3	6	173
6	111.91367	18.40822	N52W	21	3	0.2	12.6	227
7	111.91329	18.40803	N45W	35	2.5	0.1	8.8	226, 227
8	111.91308	18.40791	N35W	20	2	0.1	4	226
9	111.91324	18.40785	N38W	18	2.5	0.1	4.5	173, 227
10	111.91421	18.40782	N27W	3.5	1	0.1	0.4	173
11	111.91354	18.40770	N59E	3.5	1	0.1	0.4	227
12	111.91382	18.40769	N32W	10	3	0.3	9	173
13	111.91405	18.40766	N60E	5	1.2	0.2	1.2	173
14	111.91355	18.40765	N10W	7	2	0.2	2.8	226
15	111.91435	18.40765	N72W	12	6	0.8	57.6	173
16	111.91376	18.40760	N23W	8	3	0.2	4.8	227
17-S1	111.91346	18.40768	N45W	23	8	0.2	36.8	172, 173, 227
17-S2	111.91354	18.40753	N56W	20	6.5	1.2	156	78, 172, 173, 226, 227
17-S3	111.91365	18.40739	N37W	18	4.5	0.6	48.6	172, 173, 226, 227
18	111.91405	18.40749	N81W	5	2	0.3	3	173
19	111.91383	18.40748	N46E	4	3	0.3	3.6	226, 227
20	111.91342	18.40747	N55W	6	2	0.1	1.2	173
21	111.91386	18.40745	N30W	4	1.5	0.2	1.2	227
22	111.91392	18.40741	N46W	11	2.5	0.1	2.8	227
23	111.91387	18.40729	N43W	9	1.5	0.1	1.4	173
24	111.91494	18.40722	N80W	2	1	0.2	0.4	227
25	111.91359	18.40698	N48W	14	1.5	0.1	2.1	226
26	111.91324	18.40679	N70W	7.5	2.5	0.3	5.6	227

27	111.91347	18.40664	N25E	2.5	1.2	0.3	0.9	173
28	111.91321	18.40643	N83W	4	1.5	0.2	1.2	227
29	111.91321	18.40636	N53E	2	1.5	0.2	0.6	227
30	111.91351	18.40628	N56E	3.5	2	0.2	1.4	173
31	111.91350	18.40620	N85E	4.5	2	0.3	2.7	173
32	111.91380	18.40614	N74W	3	2	0.1	0.6	226
33	111.91375	18.40612	NS	3	0.8	0.1	0.2	226
34	111.91341	18.40612	N23W	3.5	1	0.3	1.1	173
35	111.91348	18.40611	N45W	4	1.2	0.3	1.4	173
36	111.91348	18.40597	N73W	8	1	0.2	1.6	173
37	111.91377	18.40597	N63W	6	1.2	0.2	1.4	78, 173, 226
38	111.91245	18.40526	N62E	2.5	0.8	0.1	0.2	227
39	111.91250	18.40525	N41E	4	3	0.3	3.6	227
40	111.91260	18.40523	N73E	7	2.5	0.3	5.3	227
41	111.91398	18.40376	N72W	7.5	3	0.8	18	172, 173, 226, 227
42	111.91419	18.40370	N39W	2	1	0.4	0.8	226, 227

* The suffixes S1-S4 after litter pile numbers represent the serial numbers of the segments comprising the litter piles.